SUPPLEMENTARY DATA

Zinc Uptake and Radial Transport in Roots of Arabidopsis thaliana: A Modelling Approach to Understand Accumulation

Juliane Claus[1,2], Ansgar Bohmann[1,2], and Andrés Chavarría-Krauser*[1,2]

[1]Center for Modelling and Simulation in the Biosciences, Universität Heidelberg, Heidelberg, Germany
[2]Interdisciplinary Center for Scientific Computing, Universität Heidelberg, Heidelberg, Germany

October 15, 2012

Summary

A cell-based model for the uptake and transport of zinc in roots of *Arabidopsis thaliana* and *Arabidopsis halleri* is derived. The model consists of a coupled system of ordinary differential equations describing the regulation of ZIP transporters and 1-D partial differential equations describing the transport in the symplast and apoplast. It considers, thus, the internal structure of the root tissue and couples transport phenomena with regulation networks. A system of ordinary differential equations for the xylem is also derived from a transport model and coupled via a boundary condition to the 1-D model of the apoplast.

S.1 Overview

Transport in the root is assumed to be mostly in radial direction. This allows to reduce the three dimensional problem into coupled one dimensional radially oriented problems. The structure along the radius is shown schematically in Fig. 1 of the main manuscript. The root is assumed to be composed of following cell types (from outside to inside): epidermis (ep), cortex (co), endodermis (en) and pericycle (pc). The cell layers extend from radius r_x to r_e. Surrounding the endodermis cells, a perfectly unpermeable Casparian strip (cs) at position r_c is assumed. Epidermis, cortex and endodermis cells are

---

*andres.chavarria@bioquant.uni-heidelberg.de

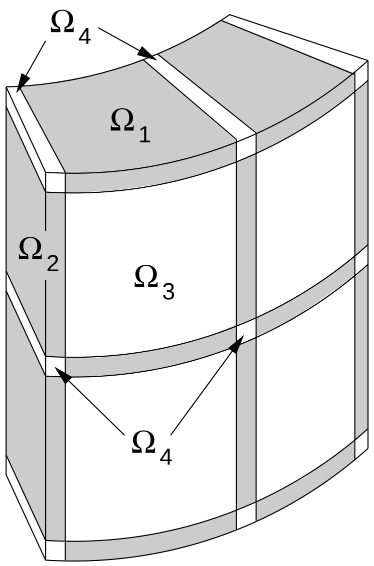

Figure S.1: Schematic drawing of the domains correspoding to apoplast Ω_1, Ω_2 and Ω_4, and symplast Ω_3. The root is assumed to be composed of a periodic assembly of such domains.

assumed to possibly have ZIP transporters (influx), while pericycle cells have only HMA4 efflux transporters. Following the results of Talke et al. [2006], the expression of *HMA4* is assumed to be independent of the zinc concentration and will be included into the model as a given efflux. Both transporters ZIP and HMA4 are assumed to be saturable and to follow Michaelis-Menten kinetics. The expression of *ZIP* in the epidermis, cortex and endodermis is allowed to adapt to the current internal zinc status based on the dimerising activator-inhibitor model proposed by Claus and Chavarría-Krauser [2012]. Depending on the average internal zinc concentration, each cell adjusts independently of the others the expression level of *ZIP*. The resulting amount of transporters is assumed to be evenly distributed on the plasma-membrane and will vary in general from cell to cell (but not within). This assumption is supported by the HMA2 expression pattern found in *A. thaliana*, Sinclair et al. [2007] (Fig. 1(c) of that publication). Note that, the model needs no other type of signal beside the internal zinc concentration. Hence, coordination is achieved merely by zinc fluxes.

To be able to reduce the problem to a system of 1-D partial differential equations, some assumptions on the geometry are needed. First, the root is best described by cylindrical coordinates and reduction will be achieved by averaging over the axial coordinate z and the azimuth φ. Second, assume that the domain of interest is made up by periodic repetition of $\bar{\Omega} := \bar{\Omega}_1 \cup \bar{\Omega}_2 \cup \bar{\Omega}_3 \cup \bar{\Omega}_4$ in azimuthal and axial direction. Here, Ω_3 denotes the symplast and Ω_1, Ω_2, and Ω_4 different parts of the apoplast respectively as indicated in Fig. S.1. And third, assume that the contribution of the apoplastic "edges" Ω_4 to the overall zinc uptake is negligible. This assumption is justified, as Ω_4 is thin compared to Ω_1 to Ω_3. Each layer of cells presented in Fig. 1 could be described by such a periodic assembly. We will assume that Ω_i, for $i = 1, \dots, 4$, span over all cell layers from r_x to r_e.

Cells have a complex internal structure with organelles, such as vacoules, nucleus, etc. They are also interconnected by plasmodesmata – channels which traverse the cell wall. To avoid the treatment of these internal structures, we treat the cell content as a porous medium with a given volume fraction, i.e. the vacoules are not treated as separate structures. Therefore, we introduce a volume fraction $\Phi = \Phi(r)$ for the symplast, which depends only on the radial position. This assumption is valid in view of the periodic structure of the cell and orientation of cell layers (Fig. 1). Cell walls are also best described as a porous medium of constant structure and porosity with constant volume fraction Ψ.

S.2 Regulation

Regulation is described by the dimerizing activator-inhibitor model proposed in Claus and Chavarría-Krauser [2012]. This leads to a system of five ordinary differential equations per cell type listed in Fig. 1

$$\left.\begin{aligned}
\frac{dG_\alpha}{dt} &= \gamma_G \left(K\, A_\alpha^2\, (1 - G_\alpha) - G_\alpha\right) \,,\\
\frac{dM_\alpha}{dt} &= \gamma_M \left(G_\alpha - M_\alpha\right) \,,\\
\frac{dT_\alpha}{dt} &= \gamma_T \left(M_\alpha - T_\alpha\right) \,,\\
\frac{dA_\alpha}{dt} &= \gamma_A \left(1 - \Gamma\, A_\alpha\, I_\alpha - A_\alpha\right) \,,\\
\frac{dI_\alpha}{dt} &= \gamma_I \left(\Gamma_I\, \zeta_\alpha - \Gamma'\, A_\alpha\, I_\alpha - (1 + \Gamma_I\, \zeta_\alpha)\, I_\alpha\right) \,,
\end{aligned}\right\} \quad \begin{aligned} &\text{for } t \in (0, \infty) \,,\\ &\alpha = en, co, ep \,, \end{aligned} \tag{S1}$$

where G_α is the gene expression level, M_α the transcript level, T_α the transporter level, A_α an activator and I_α an inhibitor, and ζ_α the internal zinc concentration. The factors γ_i, for $i = G, M, T, A, I$, are related to the time scales of each single reaction step. This system was non-dimensionalized in such a way that all variables take values between 0 and 1. Pericycle cells are not included, because these efflux cells can be assumed to not express an influx transporter. Fig. 3 in the main manuscript presents a diagram of the processes modelled by Eq. (S1).

The model expects one single value for the internal zinc concentration $\zeta_\alpha(t)$, while the transport model delivers a distribution $\mathcal{Z} = \mathcal{Z}(x,t)$ with $x \in \Omega_3$. Thus, the zinc concentration varies inside a single cell. To circumvent this issue, we assume that a cell senses the average zinc concentration inside it

$$\zeta_\alpha(t) = \zeta_0^{-1} \frac{1}{\mu(C_\alpha)} \int_{C_\alpha} \mathcal{Z}(x,t)\, dx \qquad \text{for } t \in [0, \infty),\ \alpha = en, co, ep \,, \tag{S2}$$

where ζ_0^{-1} is a scaling factor (ζ_α is non-dimensionalized), integration is over the cell $C_\alpha \subset \Omega_3$ and $\mu(C_\alpha)$ is its volume. The transporters regulated by Eq. (S1) are assumed to be distributed evenly on the surface ∂C_α of the cell, and a distribution of transporters is constructed as follows

$$\mathcal{T}(x,t) = \sum_{\alpha \in \{en,co,ep\}} T_\alpha(t)\, \chi_{\partial C_\alpha}(x) \ , \qquad \text{for } (x,t) \in \overline{\Omega}_3 \times [0,\infty) \tag{S3}$$

with the characteristic function

$$\chi_{\partial C_\alpha}(x) = \begin{cases} 1 & \text{if } x \in \partial C_\alpha \ , \\ 0 & \text{if } x \notin \partial C_\alpha \ . \end{cases}$$

HMA4 efflux transporters at the pericycle are included in a similar manner

$$\mathcal{H}(x) = H_{pc}\, \chi_{\partial C_{pc}}(x) \ , \qquad x \in \overline{\Omega}_3 \ , \tag{S4}$$

where the assumption that the level H_{pc} of HMA4 is constant was used, Talke et al. [2006].

S.3 Water flow

Before treating our main topic of zinc transport in the root, we construct a simple model for water flow. Membranes restrict the movement of zinc, but water carries it along the flow path (advection). This process influences the distribution of zinc and determines how fast variations in external zinc concentration spread in the system. Ultimatelly, advection is essential to the regulation patterns.

To avoid a complete treatment of water fluxes in root tissues, we focus only on mass conservation delivering the flow speed by consideration of effective flow cross sections. Variation of cross section in the symplast is included through the volume fraction $\Phi(r)$. Water fluxes in the apoplast are assumed to be small compared to those in the symplast and will be neglected here. This includes the assumtpion that there is no exchange between symplast and apoplast, although the apoplast is believed to contribute to the total flux, Steudle [2000]. We assume that epidermal cells take up water from the medium with a constant flux density q_0. During its pathway to the xylem, water is assumed to be conserved and to have a flow speed that depends only on volume fraction and geometry (radial convergence). This approach is very simplistic and other more sophisticated models have been proposed, for example Katou and Furumoto [1986], Katou et al. [1987], Taura et al. [1988], Katou and Taura [1989], Murphy [2000]. Modeling water fluxes in plant tissues is a complex problem which deserves treatment of its own and is out of scope of this manuscript.

Mass conservation for an incompressible fluid reads in the symplast

$$\operatorname{div}(\Phi \mathbf{v}) = 0 \qquad \text{in } \Omega_3 \ , \tag{S5}$$

where Φ is the volume fraction and $\mathbf{v}$ is the flow velocity. Eq. (S5) is expressed in cylindrical coordinates $(r,\, \varphi,\, z)$ to reflect the geometry of roots

$$\frac{1}{r}\partial_r(r\,\Phi\,v_r) + \frac{1}{r}\partial_\varphi(\Phi\,v_\varphi) + \partial_z(\Phi\,v_z) = 0\ . \tag{S6}$$

where v_r, v_φ, and v_z denote the radial, azimuthal, and axial component of the velocity $\mathbf{v}$. To the end of reducing the model to 1-D we consider the surfaces

$$\Gamma_i\,(r) := \left\{\,\mathbf{x} \in \Omega_i \;\middle|\; x_1^2 + x_2^2 = r^2\,\right\} \qquad \text{for } i = 1,\, 2,\, 3\ , \tag{S7}$$

which can be described in cylindrical coordinates by

$$(r, \varphi,\, z) \in \{r\} \times (0, \varphi_{0,i}) \times (0,\, z_{0,i}) \qquad \text{for } i = 1,\, 2,\, 3\ ,$$

with azimuth $\varphi_{0,i}$ and height $z_{0,i}$ of the considered domain. Note the use of different polar coordinate systems for Ω_1, Ω_2, and Ω_3. Let $\mu_i\,(r) = r\,\varphi_{0,i}\,z_{0,i}$ denote the area of $\Gamma_i\,(r)$. Introduce the averaged radial velocity in the symplast Ω_3

$$v(r) := \frac{1}{\mu_3\,(r)} \int_{\Gamma_3(r)} v_r(r, \varphi, z)\,\mathrm{d}\gamma\ , \qquad \text{for } r \in [r_x, r_e]\ ,$$

and consider the corresponding average of Eq. (S6) over $\Gamma_3\,(r)$:

$$\frac{1}{\mu_3(r)} \int_{\Gamma_3(r)} \frac{1}{r}\partial_r(r\,\Phi\,v_r)\,\mathrm{d}\gamma = -\frac{1}{\mu_3(r)} \int_{\Gamma_3(r)} \left(\frac{1}{r}\partial_\varphi(\Phi\,v_\varphi) + \partial_z(\Phi\,v_z)\right) \mathrm{d}\gamma\ ,$$

where the second and third terms in Eq. (S6) were moved to the right hand side. With the surface element $\mathrm{d}\gamma = r\,\mathrm{d}\varphi\,\mathrm{d}z$ the left hand side of the equation is

$$\frac{1}{\mu_3(r)} \int_{\Gamma_3(r)} \frac{1}{r}\partial_r(r\,\Phi\,v_r)\,\mathrm{d}\gamma = \frac{1}{r}\partial_r(r\,\Phi\,v)\ ,$$

while the terms on the right hand side correspond to a two dimensional divergence and can be transformed into an integral over the boundary $\partial\Gamma_i(r)$. This boundary integral is zero, based on the assumption that the apoplast and symplast do not exchange water (consequence of assuming no water fluxes in the apoplast). We obtain an equation for the average flow velocity in the symplast

$$\partial_r(r\,\Phi\,v) = 0 \qquad \text{for } r_x < r < r_e\ , \tag{S8}$$

$$\Phi v\big|_{r=r_e} = q_0\ , \tag{S9}$$

where the water influx q_0 was prescribed on the root surface ($r = r_e$). This system can be solved by integration rendering

$$v(r) = \frac{r_e}{r}\frac{q_0}{\Phi(r)} \qquad \text{for } r_x \le r \le r_e\ . \tag{S10}$$

Fig. 2 in the main manuscript shows the flow velocity used in the simulation. The volume fraction in the symplast $\Phi(r)$ considers the periodic space restriction produced by vacoules and plasmodesmata. An estimate based on Rutschow et al. [2011] delivers a volume fraction in plasmodesmata of the order of 0.15, while the vacoule was assumed to make up 80% of the cell volume ($\Phi_3 = 0.2$). Table S.2 presents the geometry parameters on which the calculations were based. This parameter set represents a typical *A. thaliana* root.

S.4 Zinc transport

Having determined the flow velocities in the compartments considered, we are able to move on to the task of finding a model for zinc. Its transport can be modelled by a diffusion advection problem, that states the conservation of zinc

$$\partial_t(\Psi\,\mathcal{Z}_i) - \operatorname{div}(\Psi\,D\,\operatorname{grad}\mathcal{Z}_i) = 0 \qquad \text{in } \Omega_i \times (0,\infty)\ ,\ i = 1, 2\ , \tag{S11a}$$

$$\partial_t(\Phi\,\mathcal{Z}_3) + \operatorname{div}(\Phi\,\mathbf{v}\,\mathcal{Z}_3 - \Phi\,D\,\operatorname{grad}\mathcal{Z}_3) = 0 \qquad \text{in } \Omega_3 \times (0,\infty)\ , \tag{S11b}$$

where Ψ is the volume fraction of the apoplasts Ω_1 and Ω_2, $\mathcal{Z}_i$ is the zinc concentration and D a diffusion coefficient. Transport in the apoplast is assumed to take place only by means of diffusion, as the water flow velocity was assumed to be zero.

S.4.1 Reduction to 1-D

Define Z_i as the average of $\mathcal{Z}_i$ over $\Gamma_i\,(r)$:

$$Z_i(r,t) := \frac{1}{\mu_i(r)} \int_{\Gamma_i(r)} \mathcal{Z}_i(x,t)\,\mathrm{d}\gamma\ , \qquad \text{for } (r,t) \in [r_x, r_e] \times [0,\infty)\ .$$

We proceed to average Eqs. (S11a) and (S11b). We will average exemplarily Eq. (S11b). The result will apply also to Eq. (S11a) by exchanging Φ with Ψ and setting $v = 0$. Treatment of the time derivative term is straightforward

$$\frac{1}{\mu_3(r)} \int_{\Gamma_3(r)} \partial_t\,(\Phi\,\mathcal{Z}_3)\ \mathrm{d}\gamma = \partial_t\,(\Phi\,Z_3)$$

The contribution of the advection term in Eq. (S11b) is

$$\frac{1}{\mu_3(r)} \int_{\Gamma_3(r)} \operatorname{div}(\Phi\,\mathbf{v}\,\mathcal{Z}_3)\,\mathrm{d}\gamma = \frac{1}{r}\,\partial_r \left(r\,\Phi\,\frac{1}{\mu_3(r)} \int_{\Gamma_3(r)} v_r\,\mathcal{Z}_3\,\mathrm{d}\gamma \right) + \frac{1}{\mu_3(r)} \int_{\partial\Gamma_3(r)} \Phi\,v_n\,\mathcal{Z}_3\,\mathrm{d}s\ ,$$

where v_n is the normal velocity on $\partial\Gamma_3(r)$. For the sake of generality the integral over $\partial\Gamma_3(r)$ is kept, although it is zero by the assumption of no water exchange between the apoplast and symplast ($v_n = 0$). By the mean value theorem, there exists a $\tilde{v}\,(r)$ so that

$$\int_{\Gamma_3(r)} v_r\,\mathcal{Z}_3\,\mathrm{d}\gamma = \tilde{v}\,(r) \int_{\Gamma_3(r)} \mathcal{Z}_3\,\mathrm{d}\gamma\ .$$

This renders the approximation

$$\frac{1}{\mu_3(r)} \int_{\Gamma_3(r)} \operatorname{div}(\Phi\,\mathbf{v}\,\mathcal{Z}_3)\,\mathrm{d}\gamma \approx \frac{1}{r}\,\partial_r\left(r\,\Phi\,v\,Z_3\right) + \frac{1}{\mu_3(r)} \int_{\partial\Gamma_3(r)} \Phi\,v_n\,\mathcal{Z}_3\,\mathrm{d}s\ ,$$

where $\tilde{v} \approx v$ was assumed. In the last step we had to make a somewhat crude approximation. However, without explicitely solving the whole 3-D problem, this is the best that can be done. The contribution of diffusion is obtained by expressing the divergence and gradient operators in cylindrical coordinates. The terms containing an r-derivative are

$$-\frac{1}{\mu_3(r)} \int_{\Gamma_3(r)} \frac{1}{r}\,\partial_r(\Phi\,D\,r\,\partial_r\mathcal{Z}_3)\,\mathrm{d}\gamma = -\frac{1}{r}\,\partial_r\left(\Phi\,D\,r\,\partial_r Z_3\right)\ .$$

The term containing φ- and z-derivatives are transformed into an integral over the boundary of $\Gamma_3(r)$

$$-\frac{1}{\mu_3(r)} \int_{\Gamma_3(r)} \left(\frac{1}{r}\,\partial_\varphi\left(\frac{\Phi\,D}{r}\,\partial_\varphi\mathcal{Z}_3\right) + \partial_z(\Phi\,D\,\partial_z\mathcal{Z}_3)\right)\mathrm{d}\gamma = -\frac{1}{\mu_3(r)} \int_{\partial\Gamma_3(r)} \Phi\,D\,\partial_n\mathcal{Z}_3\,\mathrm{d}s\ ,$$

where $\partial_n\mathcal{Z}_3$ is the normal derivative of $\mathcal{Z}_3$ on $\partial\Gamma_3(r)$. Summation of this boundary integral with the one obtained from the advection term delivers the average flux through the boundary

$$\begin{aligned} \frac{1}{\mu_3(r)} \int_{\partial\Gamma_3(r)} \Phi\,\left(v_n\,\mathcal{Z}_3 - D\,\partial_n\mathcal{Z}_3\right)\,\mathrm{d}s &= -Q_3\ , \\ Q_i &:= \sum_{j=1}^{2} \sigma_{ij}(r)\,J_j(r) \end{aligned} \tag{S12}$$

where the flux densities $J_j(r)$ represent the transport through ZIP and HMA4 (developed in next section), Q_3 denominates the source of zinc, and σ_{ij} is

$$(\sigma_{ij})(r) := \begin{pmatrix} -2/z_{0,1} & 0 \\ 0 & -2/r\varphi_{0,2} \\ 2/z_{0,3} & 2/r\varphi_{0,3} \end{pmatrix}\ . \tag{S13}$$

The sign convention of J_i is as follows: positive for a flux from the apoplast into the symplast and negative vice versa. σ_{ij} is related to the ratio of the length of the pieces composing the boundary $\partial\Gamma_3(r)$ to the area of $\Gamma_3(r)$ and weights, thus, the flux densities J_j to account correctly the change in average concentration.

Putting everything together, the following reduced model for the symplast Ω_3 is obtained

$$\partial_t(\Phi\,Z_3) + \frac{1}{r}\,\partial_r\left(r\,\Phi\,v\,Z_3 - \Phi\,D\,r\,\partial_r Z_3\right) = Q_3 \qquad \text{in } (r_x, r_e)\times(0,\infty)\ . \tag{S14}$$

It is practical for the implementation of a numerical method to rewrite the equation into a conservative form by introducing $r\,Z_i$ as a variable. Applying the results for Ω_3 to Ω_1 and Ω_2, the following system is obtained

$$\begin{aligned} \partial_t(\Psi\, rZ_1) + \partial_r\big((D/r)\,\Psi\, rZ_1 - \Psi\, D\,\partial_r(rZ_1)\big) &= r\,Q_1\ , \\ \partial_t(\Psi\, rZ_2) + \partial_r\big((D/r)\,\Psi\, rZ_2 - \Psi\, D\,\partial_r(rZ_2)\big) &= r\,Q_2\ , \qquad \text{in } (r_x, r_e)\times(0,\infty)\ . \\ \partial_t(\Phi\, rZ_3) + \partial_r\big(\,(v + D/r)\ \Phi\, rZ_3 - \Phi\, D\,\partial_r(rZ_3)\big) &= r\,Q_3\ , \end{aligned} \tag{S15}$$

Initial values and boundary conditions are developed in Section S.4.3.

S.4.2 Flux densities J_j

The zinc sources Q_i on the right hand side of Eq. (S15) depend on the flux densities J_j, which still need to be specified. The zinc flux through transporters can be modelled by a saturable pointwise reaction mechanism

$$\begin{aligned} Z_i + T &\rightleftharpoons Z{-}T \longrightarrow Z_3 + T\ , \qquad \text{for } i = 1, 2\ , \\ Z_3 + H &\rightleftharpoons Z{-}H \longrightarrow Z_i + H\ . \end{aligned}$$

We will assume that the above reactions follow Michaelis-Menten kinetics and introduce as in Claus and Chavarría-Krauser [2012] a saturation function

$$f(Z, K) = \frac{Z}{Z + K}\ , \tag{S16}$$

where K is the corresponding Michaelis-Menten constant. We introduce versions of $\mathcal{T}(x,t)$ and $\mathcal{H}(x)$ which depend on the radius by averaging over $\partial\Gamma_3(r)$

$$T(r,t) := \frac{1}{\mu\big(\partial\Gamma_3(r)\big)} \int_{\partial\Gamma_3(r)} \mathcal{T}(x,t)\,\mathrm{d}s\ , \qquad \text{for } (r,t) \in [r_x, r_e]\times[0,\infty)\ , \tag{S17a}$$

$$H(r) := \frac{1}{\mu\big(\partial\Gamma_3(r)\big)} \int_{\partial\Gamma_3(r)} \mathcal{H}(x)\,\mathrm{d}s\ , \qquad \text{for } r \in [r_x, r_e]\ . \tag{S17b}$$

Note that, $T(r,t)$ is equal to $T_{en}(t)$, $T_{co}(t)$ and $T_{ep}(t)$, respectively, for an r inside one of these cells, zero elsewhere. $H(r)$ is equal to H_{pc} for an r inside the pericycle and zero elsewhere. The reaction probability depends on $\Psi T(r,t)$ instead of only $T(r,t)$, because Ω_1 and Ω_2 are porous media and only the reduced amount $\Psi T(r,t)$ has actually contact to Z_1 and Z_2. No correction is needed for $H(r)$, as the cytoplasm can be assumed to have direct contact with the membrane, so that the complete $H(r)$ can react with Z_3.

In total, the flux densities J_j are modelled as

$$J_j(r,t) = \Phi\,T_0\,T(r,t)\,f\big(Z_j(r,t), K^t\big) - H_0\,H(r)\,f\big(Z_3(r,t), K^h\big)\ , \qquad j = 1, 2\ , \tag{S18}$$

where T_0 and H_0 are constants that characterize the true amount of transporters (non-dimensionalized regulation).

S.4.3 Initial values and boundary conditions

Equation (S15) needs initial values and suitable boundary contions to obtain a well posed (solvable) problem. The apoplast is assumed to have access to a perfectly stirred medium of concentration Z^e. A concentration $Z^x(t)$ is prescribed at the xylem. This concentration depends on the flux of zinc through HMA4 and a model will be developed in the next section. The impermeability of the Casparian strip is considered by setting a no-flux condition. In total, we prescribe for the apoplasts Ω_1 and Ω_2

$$\left.\begin{aligned} Z_i\Big|_{r=r_x} &= Z^x(t)\ , \\ (D/r)\,\Psi\, r Z_i - \Psi\, D\, \partial_r(rZ_i)\Big|_{r\nearrow r_c} &= 0\ , \\ (D/r)\,\Psi\, r Z_i - \Psi\, D\, \partial_r(rZ_i)\Big|_{r\searrow r_c} &= 0\ , \\ Z_i\Big|_{r=r_e} &= Z^e\ , \end{aligned}\right\} \quad \text{for } t \in [0,\infty),\ i = 1,2\ . \tag{S19}$$

The zinc flux is prescribed at the boundary of the symplast Ω_3

$$(v + D/r)\ \Phi\, r Z_3 - \Phi\, D\, \partial_r(rZ_3)\Big|_{r=r_x} = r\, H_0\, H_{pc}\, f\big(Z_3(r_x), K^h\big)\ , \tag{S20a}$$

$$(v + D/r)\ \Phi\, r Z_3 - \Phi\, D\, \partial_r(rZ_3)\Big|_{r=r_e} = -r\, \Phi\, T_0\, T_{ep}\, f\big(Z^e, K^t\big)\ , \tag{S20b}$$

$$\text{for } t \in [0,\infty)\ .$$

Published experimental results that capture the dynamics of regulation, focus on changes from one steady state at a given external concentration to another steady state for a different concentration (e.g. zinc resupply). Therefore, the initial conditions used here are solutions of the stationary version of Eq. (S15)

$$Z_i(r,t)\Big|_{t=0} = \overline{Z}_i(r) \qquad \text{for } r \in [r_x, r_e]\ ,\ i = 1,2,3, \tag{S21}$$

where the $\overline{Z}_i$ fulfill the following equations

$$\partial_r\big(\,(D/r)\ \Psi\, r\overline{Z}_i - \Psi\, D\, \partial_r(r\overline{Z}_i)\big) = r\, Q_i\ , \quad \text{in } (r_x, r_e) \times (0,\infty)\ ,\ i = 1,2\ , \tag{S22}$$

$$\partial_r\big(\,(v + D/r)\ \Phi\, r\overline{Z}_3 - \Phi\, D\, \partial_r(r\overline{Z}_3)\big) = r\, Q_3 \quad \text{in } (r_x, r_e) \times (0,\infty)\ , \tag{S23}$$

with boundary conditions Eqs. (S19), (S20a) and (S20b). In general, the steady state for given Z^e and q_0 will be determined, used as a initial condition, one of these parameters changed, and the dynamics of the transition captured.

S.4.4 Xylem

A calculation of the apoplastic zinc concentration in the region enclosed by the Casparian strip ($r_x \le r \le r_c$) needs the concentration of zinc in the xylem. For simplicity, we will pose a model for the central cylinder $0 \le r < r_x$ (i.e. stele without the pericycle) and account the true size of the xylem by a constant volume fraction Ψ_x. The domain describing this tissue will be denoted as Ω_x, where the x stands for *xylem*.

Eqs. (S5) and (S11b) apply also to this tissue

$$\mathrm{div}(\Psi_x \mathbf{v}_x) = 0 \qquad \text{in } \Omega_x \ , \tag{S24}$$

$$\partial_t(\Psi_x \mathcal{Z}_x) + \mathrm{div}\,(\Psi_x \,\mathbf{v}_x \,\mathcal{Z}_x - \Psi_x \,D \ \mathrm{grad}\,\mathcal{Z}_x) = 0 \qquad \text{in } \Omega_x \times (0,\infty) \ , \tag{S25}$$

where $\mathbf{v}_x$ is the flow velocity and $\mathcal{Z}_x$ is the zinc concentration in the central cylinder Ω_x. An average can be obtained as in Secs. S.3 and S.4. The main difference is that the surface over which the average is created is here

$$\Gamma_x\,(z) := \{\, \mathbf{x} \in \Omega_x \ | \, x_3 = z \,\} \ .$$

Conservation of water delivers

$$\partial_z(\Psi_x \, v_x) = -\frac{2}{r_x}\Phi(r_x)\, v(r_x) \ , \tag{S26}$$

where $\Phi(r_x)v(r_x)$ is the flow velocity of the water being delivered from the symplast, and the average velocity in the xylem is defined as

$$v_x(z) := \frac{1}{\mu\big(\Gamma_x(z)\big)} \int_{\Gamma_x(z)} v_{z,x}(r,\varphi,z)\,\mathrm{d}\gamma \ , \qquad \text{for } z \in [0,L] \ \ ,$$

where L is the length of the root portion considered. Expression of $\Phi(r_x)\,v(r_x)$ by Eq. (S10), integration of Eq. (S26), and assumption of $v_x(0) = 0$ delivers

$$v_x(z) = -\frac{2}{r_x}\frac{r_e}{r_x}\frac{q_0}{\Psi_x}\,z \qquad \text{for } z \in [0,L] \ , \tag{S27}$$

which is a linear function of z. Remeber that $q_0 < 0$ so that $v_x(z) \geq 0$ for $z \geq 0$. Eq. (S27) is based on the assumption that q_0 is constant, which will not be true in reality. The pressure gradient between the xylem and the medium will fall with z and, hence, $v_x(z)$ cannot grow linearly indefinitelly and will stagnate at a constant value. However, $v_x(z)$ will behave similar to Eq. (S27) in a region near $z = 0$. We focus on this region and assume validity of Eq. (S27).

An average for the equation describing the conservation of zinc is obtained readily

$$\partial_t(\Psi_x Z_x) + \partial_z(\Psi_x \, v_x \, Z_x - \Psi_x \, D \, \partial_z Z_x) = \frac{2}{r_x} H_0 \, H_{pc} \, f\big(Z_3(r_x,t), K^h\big) \ , \tag{S28}$$

where the boundary condition Eq. (S20a) divided by r was used and the average zinc concentration is defined as

$$Z_x(z,t) := \frac{1}{\mu\big(\Gamma_x(z)\big)} \int_{\Gamma_x(z)} \mathcal{Z}_x(x,t)\,\mathrm{d}\gamma \qquad \text{for } (z,t) \in [0,L] \times [0,\infty) \ .$$

A preliminary simulation of this equation with no-flux and open vessel conditions at $z = 0$ and $z = L$, respectivelly, shows that Z_x is almost constant in space. Hence, we set $Z_x(z,t) \approx Z^x(t)$, use that Ψ_x is constant and express v_x by Eq. (S27) to obtain

$$\begin{aligned} \frac{dZ^x}{dt} &= \frac{1}{\Psi_x}\frac{2}{r_x}\left(\frac{r_e}{r_x} q_0\, Z^x + H_0\, H_{pc}\, f\big(Z_3(r_x,t), K^h\big)\right) \qquad \text{for } t \in (0,\infty)\ , \\ Z^x\big|_{t=0} &= Z^x_0\ . \end{aligned} \tag{S29}$$

Note again that $q_0 < 0$, so that this equation has a non-trivial positive steady state solution

$$\overline{Z}^x = -\frac{r_x}{r_e}\frac{H_0\, H_{pc}}{q_0}\, f\big(\overline{Z}_3(r_x), K^h\big)\ . \tag{S30}$$

References

J. Claus and A. Chavarría-Krauser. Modeling regulation of zinc uptake via ZIP transporters in yeast and plant roots. *PLoS One*, 7:e37193, 2012.

N. Grotz, T. Fox, E. Connolly, W. Park, M.L. Guerinot, and D.J. Eide. Identification of a family of zinc transporter genes from *Arabidopsis* that respond to zinc deficiency. *PNAS*, 95:7220–7224, 1998.

K. Katou and M. Furumoto. A mechanism of respiration-dependent water uptake in higher plants. *Protoplasma*, 130:80–82, 1986.

K. Katou and T. Taura. Mechanism of pressure-induced water flow across plant roots. *Protoplasma*, 150:124–130, 1989.

K. Katou, T. Taura, and M. Furumoto. A model for water transport in the stele of plant roots. *Protoplasma*, 140:123–132, 1987.

R. Murphy. Some compartmental models of the root: steady state behavior. *J. Theor. Biol.*, 207:557–576, 2000.

H. Rutschow, T. Baskin, and E. M. Kramer. Regulation of solute flux through plasmodesmata in the root meristem. *Plant Physiol.*, 155:1817–1826, 2011.

S.A. Sinclair, S.M. Sherson, R. Jarvis, J. Camakaris, and C.S. Cobbett. The use of the zinc-fluorophore, Zinpyr-1, in the study of zinc homeostasis in *Arabidopsis* roots. *New Phytol.*, 174:39–45, 2007.

E. Steudle. Water uptake by plant roots: an integration of views. *Plant Soil*, 226:45–56, 2000.

I.N. Talke, M. Hanikenne, and U. Krämer. Zinc-dependent global transcriptional control, transcriptional deregulation, and higher gene copy number for genes in metal homeostasis of the hyperaccumulator *Arabidopsis halleri*. *Plant Physiol.*, 142:148–167, 2006.

T. Taura, Y. Iwaikawa, M. Furumoto, and K. Katou. A model for radial water transport across plant roots. *Protoplasma*, 144:170–179, 1988.

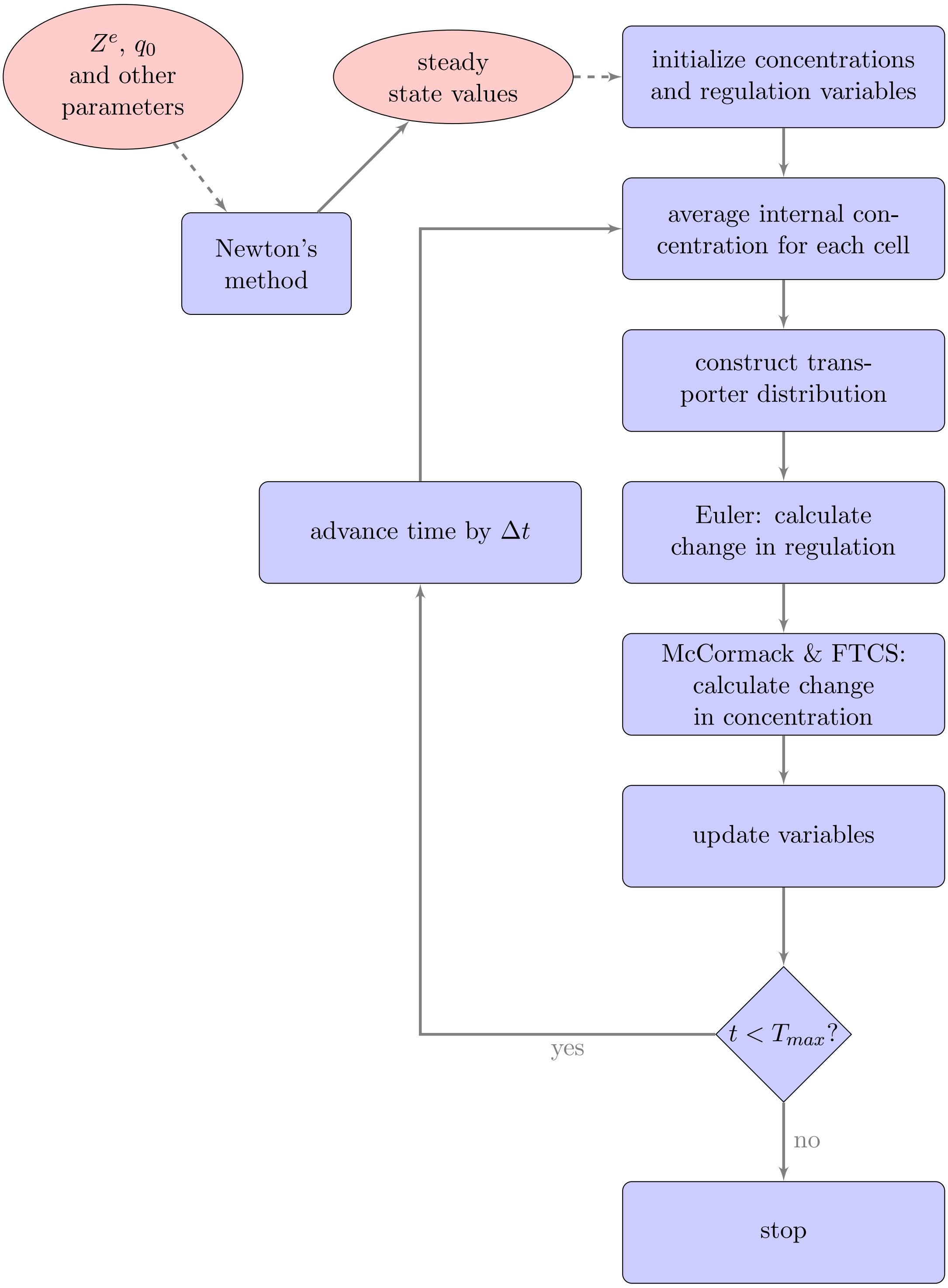

Figure S.2: Diagram of the steps involved in coupling the numerical schemes.

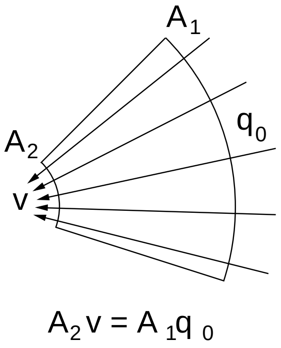

Figure S.3: Schematic diagram of effect of cylindrical geometry on water flow velocity. The flow cross section becomes smaller for smaller radii resulting in acceleration of the flow: $v = \frac{A_1}{A_2} q_0 > q_0$ for $A_1 > A_2$.

Table S.1: Parameters used in the regulation model. Values taken from Claus and Chavarría-Krauser [2012]

Parameter	K^{t*}	K	Γ	Γ'	Γ_I	γ_G	γ_M	γ_T	γ_A	γ_I
Value	13 μM	20	38	167.2	1000	4	4	1	1	1

* Value for ZIP1, Grotz et al. [1998]

Table S.2: Geometry parameters used in the simulation. These correspond to a typical *Arabidopsis thaliana* root.

Parameter	r_x	r_c	r_e	$z_{0,1}$	$z_{0,3}$	$\phi_{0,3}$
Value	6 μm	12.5 μm	40 μm	0.5 μm	135 μm	$\pi/10$

Table S.3: Further parameters used in the simulation.

Parameter	Value	Description
K^h	1 μM	Michaelis-Menten constant for HMA4
ζ_0	166.67 μM	Scaling factor that dimensionalizes the internal zinc concentration